

STUDY OF THE ENHANCEMENT IN THE  $\Lambda p$  INVARIANT MASS NEAR THE  $\Sigma N$  THRESHOLD  
IN  $K^-d \rightarrow \Lambda p \pi^-$  INTERACTIONS AROUND 1.0 GeV/c\*

Gideon Alexander, Bronwyn H. Hall, Nathan Jew, and George Kalmus

Department of Physics and Lawrence Radiation Laboratory, University of California, Berkeley, California 94720

and

Anne Kernan

Department of Physics, University of California, Riverside, California 92507

(Received 20 January 1969)

Data are presented for the reaction  $K^-d \rightarrow \Lambda p \pi^-$  at 910, 1007, and 1106 MeV/c in which the proton momentum is greater than 250 MeV/c. The  $\Lambda p$  invariant-mass plot shows an enhancement at about 2130 MeV, similar to that found by Cline, Laumann, and Mapp. No enhancement is seen at about 1440 MeV in the  $\Lambda \pi$  invariant mass. A simple two-step process describes our data as well as those of Cline, Laumann, and Mapp without the use of resonances.

In the absence of readily available hyperon beams, the study of the hyperon-proton ( $Y-p$ ) system in final-state interactions may be useful in the search for strangeness  $-1$ , dibaryon resonant states. Several possible  $\Lambda p$  resonances have been reported in the past; however, none has been substantiated by further investigations.<sup>1</sup> Recently Cline, Laumann, and Mapp have observed an enhancement in the  $\Lambda p$  invariant-mass distribution in a study of  $K^-d$  interactions at 400 MeV/c leading to the final state  $\Lambda p \pi^-$  with a fast proton.<sup>2</sup> This enhancement, which was centered a few MeV below the  $\Sigma N$  threshold, suggested to them the existence of a  $(\Sigma N)_{1/2}$  bound state coupled to the open  $\Lambda p$  channel, which in turn implies an elastic  $\Lambda p$  resonance with a mass of 2126 MeV and a width of less than 10 MeV. Cline, Laumann, and Mapp also observed in the same reaction a strong enhancement in the  $\Lambda \pi^-$  system at 1440 MeV.<sup>3</sup>

In this Letter we present data on the reaction

$$K^-d \rightarrow \Lambda p \pi^- \quad (1)$$

around 1 GeV/c in which the proton has a momentum greater than 250 MeV/c. We also discuss a simple model which can explain our data and those of Refs. 2 and 3 without invoking any resonances.

The experiment used pictures taken in the Lawrence Radiation Laboratory 25-in. bubble chamber filled with deuterium and exposed to a  $K^-$  beam at momenta of 910 MeV/c ( $54 \times 10^3$  pictures), 1007 MeV/c ( $12 \times 10^3$  pictures), and 1106 MeV/c ( $86 \times 10^3$  pictures). The film was scanned for two-prong events plus an associated  $V^0$ . The positive prong had to have a range greater than 5 cm in space (corresponding to a minimum proton momentum 225 MeV/c) and ionization consis-

tent with a proton. The events were then measured and kinematically fitted to the various possible final states involving  $K^0$ ,  $\Lambda$ , or  $\Sigma^0$ . No difficulty was found in separating the  $\Lambda$  or  $\Sigma^0$  from the  $K^0$ . A lower cutoff momentum of 250 MeV/c was imposed on the proton in the final state  $\Lambda^0(\Sigma^0)p\pi^-$  in order to obtain a sample of events in which both nucleons in the deuteron were involved in the interaction. From a previous study of the reaction  $K^-d \rightarrow \Lambda p \pi^- p_s$  (spectator), we estimate that the background from this reaction in our study is 20%.<sup>4</sup> The proton momentum cut in the data of Cline et al. was 150 MeV/c.<sup>5</sup>

A total of 324 events fitted the  $\Lambda p \pi^-$  hypothesis, 421 events fitted the  $\Sigma^0 p \pi^-$  hypothesis, and an additional 367 events were ambiguous between the two hypotheses. The ambiguous events were fitted by the hypothesis  $K^-d \rightarrow \Lambda \gamma p \pi^-$ . The  $\Lambda \gamma$  invariant-mass distribution had two peaks, one near the  $\Lambda$  mass and the other near the  $\Sigma^0$  mass. We accepted the 241 events in the lower mass peak as  $K^-d \rightarrow \Lambda p \pi^-$ , the cut being  $M(\Lambda \gamma) < 1165$  MeV. These 241 events together with the 324 unambiguous ones constituted our sample of 565  $\Lambda p \pi^-$  events. In the following analysis we have combined the data at the three incident  $K^-$  momenta. We discuss first the  $\Lambda p$  invariant-mass distribution and later the  $\Lambda \pi^-$  system.

Figures 1(a) and 1(d) show the  $\Lambda p$  mass plots for our data and, for comparison, those of Ref. 2, the shaded events having  $\cos(\theta_{K-\pi^-}) > 0.8$ , where  $\theta_{K-\pi^-}$  is the angle between the  $K^-$  and  $\pi^-$  in the  $K^-d$  c.m. system. This cut was applied by Cline, Laumann, and Mapp and is discussed later. Figures 1(b), 1(e), 1(c), and 1(f) show the ratios  $(F-B)/(F+B)$  and  $(P-E)/(P+E)$ , respectively, for the events in the shaded portion of histogram 1(a) and 1(d);  $F$  and  $B$  refer to the

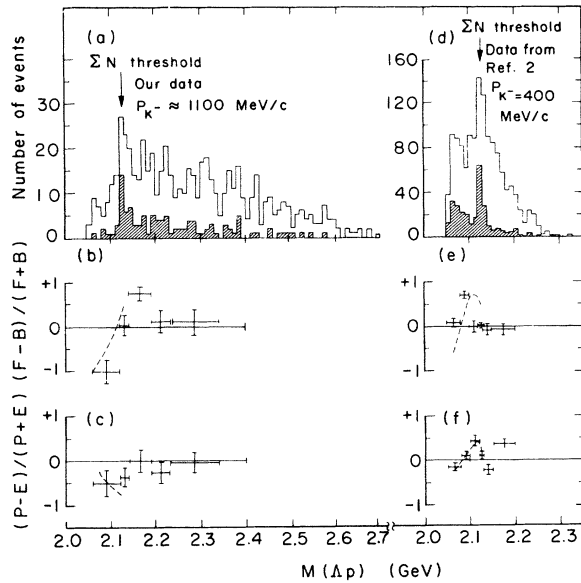


FIG. 1.  $\Lambda p$  invariant mass and  $\Lambda$  angular distributions for the reaction  $K^- d \rightarrow \Lambda p \pi^-$ . (a), (d)  $M(\Lambda p)$  distributions of our data and of the data given in Ref. 2. (b), (e)  $(F-B)/(F+B)$  as a function of  $M(\Lambda p)$ . (c), (f)  $(P-E)/(P+E)$  as a function of  $M(\Lambda p)$ . Dashed curves represent the expected distribution from the one-step process  $K^- d \rightarrow \Lambda \pi^- p_s$ .

number of forward and backward  $\Lambda$ 's in the  $\Lambda p$  rest system, and  $P$  and  $E$  refer to the number of events having  $|\cos(\theta_\Lambda)| > 0.5$  and  $|\cos(\theta_\Lambda)| < 0.5$ , respectively, where  $\theta_\Lambda$  is the angle in the  $\Lambda p$  c.m. system between the  $\Lambda$  and the line of flight of the  $\Lambda p$  system.

Figure 1(a) shows a small enhancement in the shaded histogram around 2130 MeV close to the  $\Sigma N$  threshold. [The mass resolution at  $M(\Lambda p) \approx 2130$  MeV was found to be  $\approx 3$  MeV.] Figures 1(b) and 1(c) show that, at the enhancement, the angular distribution is consistent with isotropy, while below it a deviation from isotropy is indicated. The enhancement in the  $\Lambda p$  mass plot as well as the angular distributions at this enhancement are very similar to those reported in Ref. 2 and shown in Figs. 1(d)-1(f); however, the peak in the mass plot for the 1100-MeV/c data appears to be less pronounced than that for 400 MeV/c.

In view of our results and those at 400-MeV/c incident momentum, it is of interest to investigate the extent to which one is compelled to introduce the existence of a  $\Lambda p$  resonance.<sup>6</sup> To this end we have calculated the  $\Lambda p$  invariant-mass distribution in the framework of a simple two-step process without invoking any  $YN$  resonances.<sup>7</sup>

The two-step processes considered were

$$(a) K^- d \rightarrow \Sigma^+ \pi^- (n_s) \quad (b) \Sigma^+ n_s \rightarrow \Lambda p \quad (2)$$

$$\rightarrow \Sigma^0 \pi^- (p_s) \quad \Sigma^0 p_s \rightarrow \Lambda p \quad (3)$$

$$\rightarrow \Lambda \pi^- (p_s) \quad \Lambda p_s \rightarrow \Lambda p \quad (4)$$

$$\rightarrow K^- p (n_s) \quad K^- n_s \rightarrow \Lambda \pi^- \quad (5)$$

We have also considered the process

$$K^- d \rightarrow \Lambda \pi^- p_s, \quad (6)$$

where the momentum of the spectator proton is in the tail of the Fermi momentum distribution; these events contribute mainly below  $\Sigma N$  threshold.

In order to calculate the  $M(\Lambda p)$  distribution from Reactions (2)-(4) [Reactions (5) and (6) do not contribute to a peak in  $M(\Lambda p)$ ], we have assumed that they can each be approximately described by two successive, well-separated reactions,  $KN \rightarrow Y\pi$  and then  $YN \rightarrow \Lambda p$ . This simple approach is expected to describe the processes at least qualitatively, since the deuteron is a rather loosely bound system.

The calculations have been carried out by generating individual events by a Monte Carlo method according to the two-stage reactions described above for  $K^-$  incident momenta of 400 and 1100 MeV/c, from where the bulk of the present data came.

In the first stage we have calculated the reaction  $K^- N \rightarrow Y\pi$  in the framework of the impulse model, taking into account the momentum distribution of the nucleon as given by the Hulthén wave function and using an isotropic angular distribution of the nucleons in the deuteron c.m. system. The angular distribution of the emerging hyperons was taken from known  $KN \rightarrow Y\pi$  single-nucleon interaction data at 400 and 1100 MeV/c.<sup>4,8,9</sup>

The second stage involves calculation of the relative probability for the hyperon to have a subsequent interaction with the spectator nucleon. In calculating this probability we have assumed an  $s$ -wave energy-independent matrix element for the reaction  $YN \rightarrow \Lambda p$ . Taking into account the phase-space and flux factors, the cross section is given by the expression<sup>10</sup>

$$\sigma(YN \rightarrow \Lambda p) \propto \frac{\epsilon_Y \epsilon_N \epsilon_\Lambda \epsilon_p P_f}{M^2(\Lambda p) P_i}, \quad (7)$$

where  $\epsilon_Y$ ,  $\epsilon_N$ ,  $\epsilon_\Lambda$ , and  $\epsilon_p$  are the energies of the corresponding particles and  $P_f$  and  $P_i$  are the final and initial momenta in the  $YN$  c.m. system.

This expression is in agreement with experimental data on low-energy hyperon-nucleon scattering.<sup>1</sup> We are justified in using it here, since the experimental cut of  $\cos(\theta_{K-\pi^-}) > 0.8$  restricts the momentum of the hyperon to  $\leq 250$  MeV/c and  $\leq 500$  MeV/c at  $K^-$  momenta of 400 MeV/c and 1.1 GeV/c, respectively.

The probability for the (b) reactions to occur also depends on the spatial configuration of the deuteron and, therefore, on the Fermi momentum. So, in general, the cross section in Eq. (7) should be weighted by some function  $G(P_F)$  of the Fermi momentum. However, by performing the calculations at a series of unique nucleon momenta, we have verified that the shape of the Monte Carlo mass distribution is essentially independent of the nucleon momentum. This independence comes about because  $P_Y > P_F$ , and hence  $P_i$  in Eq. (7) is not strongly correlated with  $P_F$ . Since we are interested in shape rather than absolute cross section for various final-state configurations, we can ignore the  $G(P_F)$  factor.

It is clear that any calculation in which all the particles in the reaction  $\Sigma N \rightarrow \Lambda p$  (second stage) are on the mass shell cannot generate a  $\Lambda p$  mass below  $\Sigma N$  threshold. However, since neither the  $\Sigma$  nor the  $N$  need be on the mass shell, this reaction can lead to a  $\Lambda p$  mass below  $\Sigma N$  threshold. In order to estimate the effect with the mass of the nucleon off the mass shell we constrained the total energy of the nucleons to be the mass of the deuteron, letting the masses of the two nucleons go off the mass shell in equal amounts, i.e.,

$$M_N = [\frac{1}{4}M_d^2 - P_F^2]^{1/2},$$

where  $P_F$  is the Fermi momentum and  $M_d$  is the mass of the deuteron. The other particles were taken as being of the mass shell.

The results of these calculations show that the width of the peak in the  $\Lambda p$  mass plot remains essentially unchanged, but its position shifts towards lower masses by a few MeV when the nucleons are off the mass shell. We have introduced into these calculations the same cutoffs on the momentum of the proton as were used in the experimental data, i.e., 150 and 250 MeV/c for incident  $K^-$  momenta of 400 and 1100 MeV/c, respectively.

The Monte Carlo distributions are shown in

Fig. 2 (solid curves); the dashed curves are the distributions obtained with the cut of  $\cos(\theta_{K-\pi^-}) > 0.8$ . This cut was introduced by Cline, Lauermann, and Mapp to enhance the  ${}^3S_1$  state (same as deuteron state) over the  ${}^1S_0$  state for the intermediate  $\Sigma^+n$  system.

As seen in Fig. 2, Reactions (2) and (3) generate peaks in the  $\Lambda p$  mass at  $K^-$  momenta 400 and 1100 MeV/c. The position and width of the peak from Reaction (2) at  $P_K = 400$  MeV/c correspond closely to those observed. At  $P_K = 1100$  MeV/c, the generated peak is at the observed position but is somewhat wider than that observed. The occurrence of the peak can be readily understood as arising from a combination of two factors: (1) strong production of low energy  $\Sigma$ 's in Reactions (2a) and (3a) [enhanced by the cut of  $\cos(\theta_{K-\pi^-}) > 0.8$ ], and (2) the approximate  $1/P_i$  dependence of the cross section for the exothermic Reactions (2b), (3b), and (5b) at low energy.

The  $\Lambda p$  mass plot can be adequately described at 400 and 1100 MeV/c by a suitable combination of Reactions (2)-(4) except for the region above  $\sim 2450$  MeV for the 1100-MeV/c data. The events above this mass can be explained by Reaction (5) and also the reaction  $K^-d \rightarrow \Lambda\pi^-p_S$  with a subsequent  $\pi p_S$  elastic scattering which contributes to the cross section at the high masses.

In the framework of this model one expects an isotropic  $\Lambda$  angular distribution at the  $\Sigma N$  threshold. Above threshold, without further assumption on the relative magnitudes of the various reactions, we are unable to calculate the angular

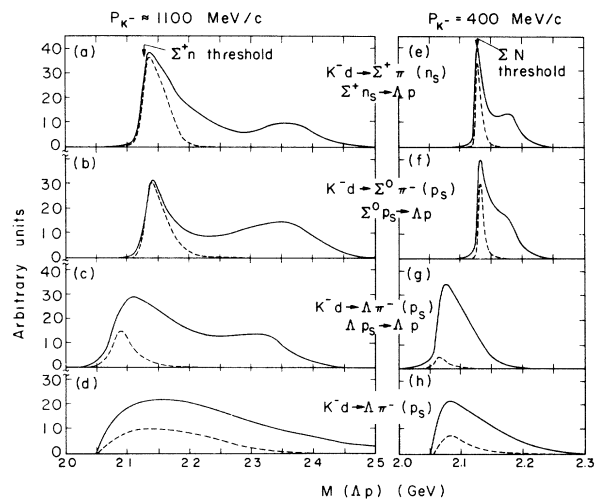


FIG. 2. Calculated  $M(\Lambda p)$  distributions for incident  $K^-$  momenta of 1100 and 400 MeV/c of the Reactions (2)-(4) and (6). The dashed curves represent the calculated distributions with  $\cos(\theta_{K-\pi^-}) > 0.8$ .

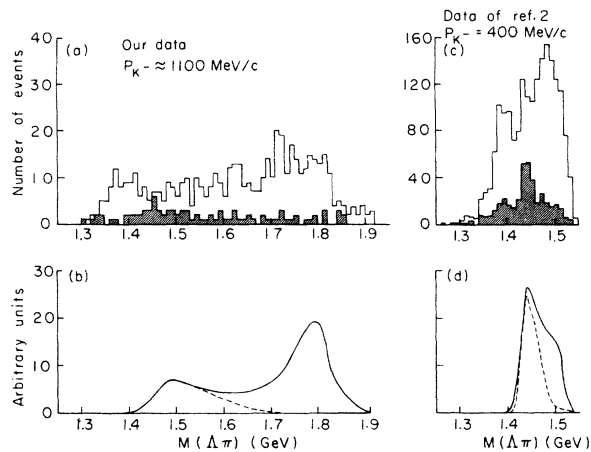


FIG. 3. Experimental and calculated  $M(\Lambda\pi)$  distributions of our data and of the data given in Ref. 2. (a), (c) Experimental  $M(\Lambda\pi)$ ; shaded area corresponds to events with  $\cos(\theta_{K^-p}) > 0.5$ . (b), (d) Calculated  $M(\Lambda\pi)$  distributions from the two-step process (5); dashed curves represent the calculated distributions with  $\cos(\theta_{K^-p}) > 0.5$ .

distributions. However, it is interesting to note that the  $\Lambda$  angular distribution below  $\Sigma N$  threshold is approximately described by the one-step process  $K^-d \rightarrow \Lambda\pi^-(p_s)$  [curves on Figs. 1(b) and 1(c)], where the spectator proton momentum is greater than the cutoff value.

Next we consider the  $\Lambda\pi$  invariant-mass distribution, shown in Fig. 3(a) for events lying outside the  $\Lambda p$  peak [ $2120 \text{ MeV} < M(\Lambda p) < 2140 \text{ MeV}$ ] and for  $\cos(\theta_{K^-p}) > 0.5$  (shaded portion), where  $\theta_{K^-p}$  is the angle between the  $K^-$  proton in the c.m. system of  $K^-d$ . The data from Ref. 3 at 400 MeV/c are shown in Fig. 3(c). There is no significant enhancement at 1440 MeV in our data.

Figures 3(b) and 3(d) show the  $\Lambda\pi^-$  mass distribution calculated for the two-step process (5). The calculation was done using the Monte Carlo method with the assumptions outlined earlier. The experimental data on  $K^-p$  elastic scattering were used in the first step,<sup>8,11</sup> and for Reaction (5b) we again assumed that the matrix element was  $s$  wave and energy independent. Reaction (5) is seen to give rise to a peak around 1440 MeV/c for incident momentum of 400 MeV/c, but not for 1100 MeV/c. Again, the peak in the 400-MeV/c data can be understood in terms of strong production of low-momentum  $K^-$  in Reaction (5a), followed by the exothermic Reaction (5b) at low energy. In  $K^-p$  elastic scattering at 1100 MeV/c

the  $K^-$  is scattered predominantly with low momentum transfer, and so the  $K^-n$  system is not formed close to threshold energy in Reaction (5b).<sup>11</sup>

Since our calculations show that the present data can be explained satisfactorily without the need for either a  $\Sigma n$  bound state or a  $\Lambda\pi$  resonance, other reactions that are sensitive to these effects should be examined. In looking for  $YN$  resonance below  $\Sigma n$  threshold two reactions may be studied: (a) free  $\Lambda p$  scattering; the rather meager data available at the  $\Sigma N$  threshold ( $p_\Lambda \approx 635 \text{ MeV}$ ) show no peak; and (b) free  $\Sigma p$  scattering; again the data are very meager and do not allow one to measure the scattering length.

\*Work supported by the U. S. Atomic Energy Commission.

<sup>1</sup>See, for example, the review by G. Alexander and U. Karshon, in High Energy Physics and Nuclear Structure, edited by G. Alexander (North-Holland Publishing Company, Amsterdam, the Netherlands, 1967), p. 36, and references therein.

<sup>2</sup>D. Cline, R. Laumann, and J. Mapp, Phys. Rev. Letters **20**, 1452 (1968).

<sup>3</sup>D. Cline, R. Laumann, and J. Mapp, Phys. Rev. Letters **21**, 1372 (1968).

<sup>4</sup>W. M. Smart, University of California Lawrence Radiation Laboratory Report No. UCRL-17712, 1967 (unpublished).

<sup>5</sup>D. Cline (University of Wisconsin), private communication.

<sup>6</sup>I. R. Kenyon, A. E. Sichirollo, and C. R. Sun, Phys. Rev. **165**, 1445 (1968). These authors also observed a peak in the  $\Lambda p$  system below  $\Sigma n$  threshold in the reaction  $K^-He^4 \rightarrow p d \Lambda^0 \pi^-$  but did not ascribe it to a  $\Sigma n$  bound state.

<sup>7</sup>Cline, Laumann, and Mapp in their papers (Refs. 2 and 3) mentioned the possibility that peaks could occur in the mass plots due to kinematic effects of the type we discuss here, but no quantitative calculations were presented.

<sup>8</sup>M. B. Watson, M. Ferro-Luzzi, and R. D. Tripp, Phys. Rev. **131**, 2248 (1963).

<sup>9</sup>R. B. Bell, Phys. Rev. Letters **19**, 936 (1967).

<sup>10</sup>See, for example, W. S. C. Williams, An Introduction to Elementary Particles (Academic Press, Inc., New York, 1961), p. 93, from which we obtain this expression for the cross section by noting that  $(\epsilon_Y + \epsilon_N) = (\epsilon_\Lambda + \epsilon_p) = M(\Lambda p)$ .

<sup>11</sup>R. Armenteros, P. Baillon, C. Brieman, M. Ferro-Luzzi, D. E. Plane, N. Schmitz, E. Burkhardt, H. Filthuth, E. Kluge, H. Oberlack, R. R. Ross, R. Barloutaud, P. Granet, J. Meyer, J. P. Porte, and J. Prevost, Nucl. Phys. **B8**, 195 (1968).